Supplemental Methods:

Breeding strategy to produce *Pparg*-/-^{epi} and WT sibling controls.

Mice containing a Cre recombinase driven by a cytokeratin 14 promoter (Tg(KRT14-cre)1Amc/J) and mice containing loxP sites flanking exons 1 & 2 of the *Pparg* allele (B6.129-*Pparg*^{tm2Rev}/J) were purchased from the Jackson Laboratory (Bar Harbor, Maine). Both mouse strains were backcrossed into the SKH1 mouse strain for 6 generations. To generate both conditional knockouts and WT sibling controls, 6th generation SKH-1 mice hemizygous for the floxed *Pparg* allele (*Pparg*(f/wt)) were crossed with 6th generation SKH-1 backcross mice hemizygous for the KRT14-Cre allele (KRT14-Cre(+/-)). Double hemizgyous pups (*Pparg*(f/wt)/ KRT14-Cre(+/-)) were then selected and crossed. In this next generation, pups that had the genotype *Pparg*(f/f)/KRT14-Cre(+/-) or *Pparg*(f/f)/KRT14-Cr(-/-) were then selected. These were then crossed to generate conditional knockouts (*Pparg*(f/f)/KRT14-Cre(+/-)) or wildtype sibling controls (*Pparg*(f/f)/KRT14-Cre(-/-)). Given that the presence or absence of the KRT14-Cre recombinase differentiates WT from conditional knockouts, all experimental mice were genotyped twice, both prior to and after experimental use to verify the presence or absence of the KRT14-Cre allele.

Detailed description of chronic UVB irradiations.

For all UVB studies, the UVB intensity was measured at a set distance prior to each experiment using a IL1700 radiometer equipped with a SED240 UVB detector (International Light, Newburyport, MA). The time of exposure for irradiation was calculated from the intensity (fluence) of the lamp and the required UVB dose. For chronic UVB studies, each cage was rotated to a different lamp location for each successive irradiation to avoid variations in fluence across the lamp length,.

Modified Tumor Classification Scheme.

Briefly, modifications to the grading of stage 1-3 microinvasive squamous cell carcinomas (MISCC) were as follows: Stage 1 MISCC showed definite invasion into the dermis but no invasion into the dermal fat layer while stage 2 MISCC had invasion into the dermal fat layer. Stage 3 MISCC showed invasion adjacent to but not into the panniculus carnosus. Invasive squamous cell carcinomas showed invasion into or through the panniculus carnosus. Given the extensive field changes in the *Pparg*-/-^{epi} mice, it was difficult at times to separate individual tumors for classification purposes. When evaluating the slides, additional tumors were not assigned unless there was a distinct change in appearance of the tumors in adjacent areas (i.e. two papillomas immediately adjacent to one another but each with its own distinct appearance and clearly two separate growths), a change in stage (i.e. stage 1 adjacent to a stage 2) or growths with an intervening benign appearing epidermis.

Topical GW9662 treatments.

The dorsal epidermis of SKH-1 mice was treated with 100 µl of 1, 10, or 100 nanomoles (nmoles) of GW9662 solubilized in 70% propylene glycol:30% ethanol for 1.5 hours prior to UVB irradiation. Prior to irradiation, the dorsal skin was wiped gently 4 times with cotton swabs soaked in 100% ethanol to remove non-absorbed reagents. Immediately following irradiation, 50 µl of GW9662 (0.5, 5 or 50 nmole) was reapplied to the dorsal skin of the mouse (total additive dose between the pre- and post-treatment = 1.5, 15 or 150 nmoles). For the 72 hour time point, 50 µl of vehicle or GW9662 (0.5 or 5 nmole) was reapplied to the dorsal epidermis daily (24 and 48 hrs) for each respective treatment group (total cumulative dose over 72 hrs = 2.5 or 25 nmoles).

Tissue cytometric analysis.

Tissue cytometric analysis was by done by first identifying individual cell nuclei by DAPI staining. Mean cell intensity for FITC labeling was used to identify epidermal (cytokeratin +) and dermal (cytokeratin neg) cells (supplemental figure 5B). Finally, cells double positive for Ki67 or p53 and pan-cytokeratin were identified using user-defined cutoffs and verified by back-directional gating (see supplemental figure 5C & D). Image analysis was done on at least 7 random 200x fields from each mouse.

Supplemental Figure 1: Loss of epidermal PPARγ results in a trend towards a greater percentage of small tumors (<2 mm) and a reduced percentage of intermediate and large tumors. Tumor sizes after 24 weeks of UVB treatment were separated into the bin size distributions shown based on the greatest tumor diameter. For each mouse, the number of tumors of each bin as a percentage of that mouse's total tumor count were calculated, then the mean ± SEM were calculated for each genotype. The *Pparg*-/-^{epi} mice exhibited a strong statistical trend towards an increased percentage of smaller tumors (1-2 mm bin size) (p=0.056, 2-tailed t-test). By 2-way ANOVA, the interaction between genotype and the three different tumor bin sizes was significant (p = 0.0128).

Supplemental Figure 2: Representative images of *Pparg*-/-^{epi} mice showing increased Ki67 immunolabeling after 24 weeks of chronic UVB irradiation. Immunofluorescent staining was performed for Ki67 (Red) and for pan-cytokeratin (Green), with DAPI counterstain (Blue). Merged images of photomicrographs taken at 200x magnification are shown for (A) Non-irradiated WT. (B) Non-irradiated *Pparg*-/-^{epi}. (C) UVB-irradiated WT. (D) UVB-irradiated *Pparg*-/-^{epi} mouse skin. Quantitation of Ki67 immunolabeling is shown in figure 3A.

Supplemental Figure 3: Representative images of *Pparg*-/-^{epi} mice showing increased positivity for p53 following 24 weeks of UVB irradiation. Immunofluorescence double labeling for p53 (Red) and pan-cytokeratin (Green), with DAPI (Blue) counterstain. Merged images of photomicrographs taken at 200x magnification are shown for: (A) UVB-irradiated WT. (B) UVB-irradiated *Pparg*-/-^{epi}. (C) Grayscale image of the p53+ immunolabeling from panel (A). (D) Grayscale image of the p53+_immunolabeling from panel (B). Non-irradiated skin was negative for p53+ (not shown). Quantitation of p53 immunopositivity is shown in figure 3B.

Supplemental Figure 4: Depiction of the tissue cytometric analysis. (A) UVB-irradiated *Pparg*-/-^{epi} skin section double labeled for p53 (Alexa Fluor 594-Red) and a FITC-conjugated pan-cytokeratin antibody (Green) as described in Methods. Nuclei were then counterstained with DAPI (Blue). (B) Using tissue cytometric analysis software, cell nuclei were detected by DAPI staining and DAPI positive nuclei were assessed for colabeling for median DAPI intensity (x-axis) and FITC (y-axis). The cutoff defined the pan-cytokeratin positive (epidermis) from the pan-cytokeratin negative (dermal) cells. (C) Scattergram showing double-labeling cutoffs for FITC (pan-cytokeratin; x-axis) and Alexa Fluor 594 (TR, p53+; y-axis). (D) Backgating of FITC+TR double positive cells to show localization in the p53+ unmerged image.

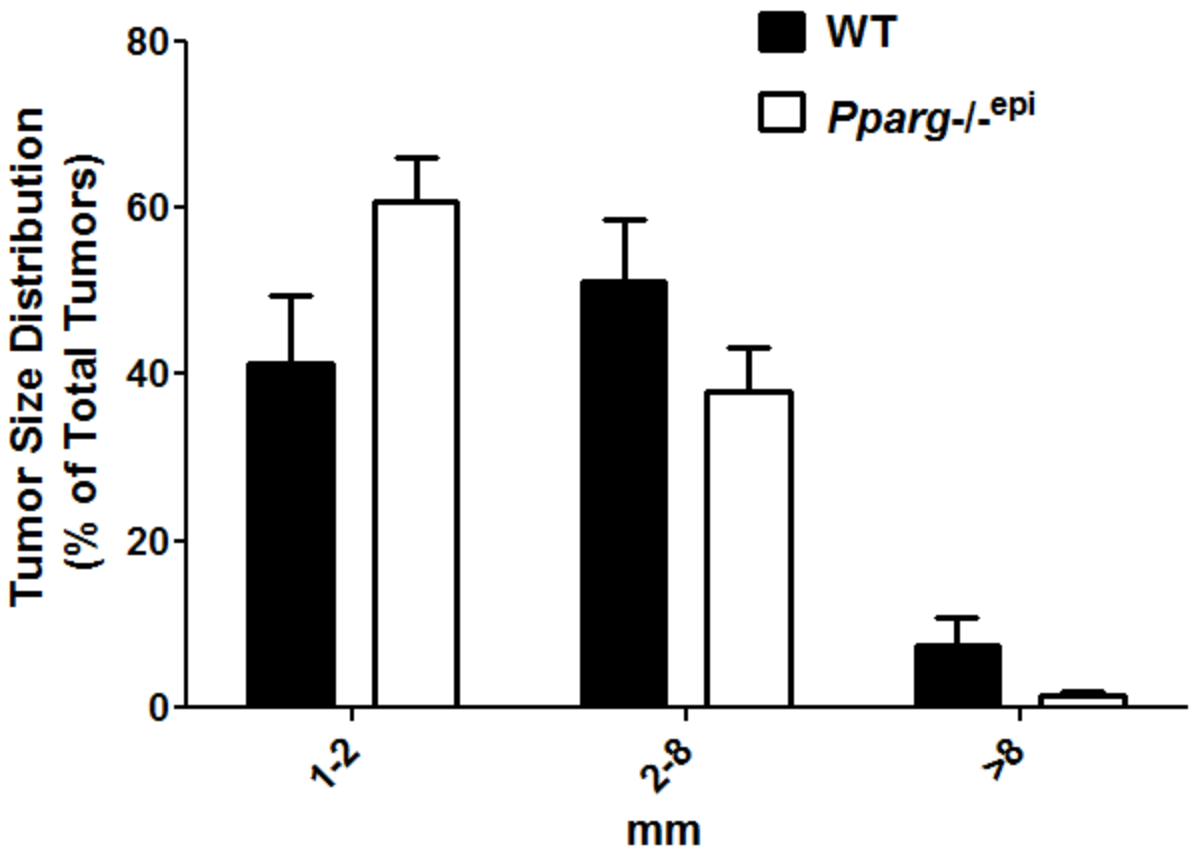

Supplemental figure 1

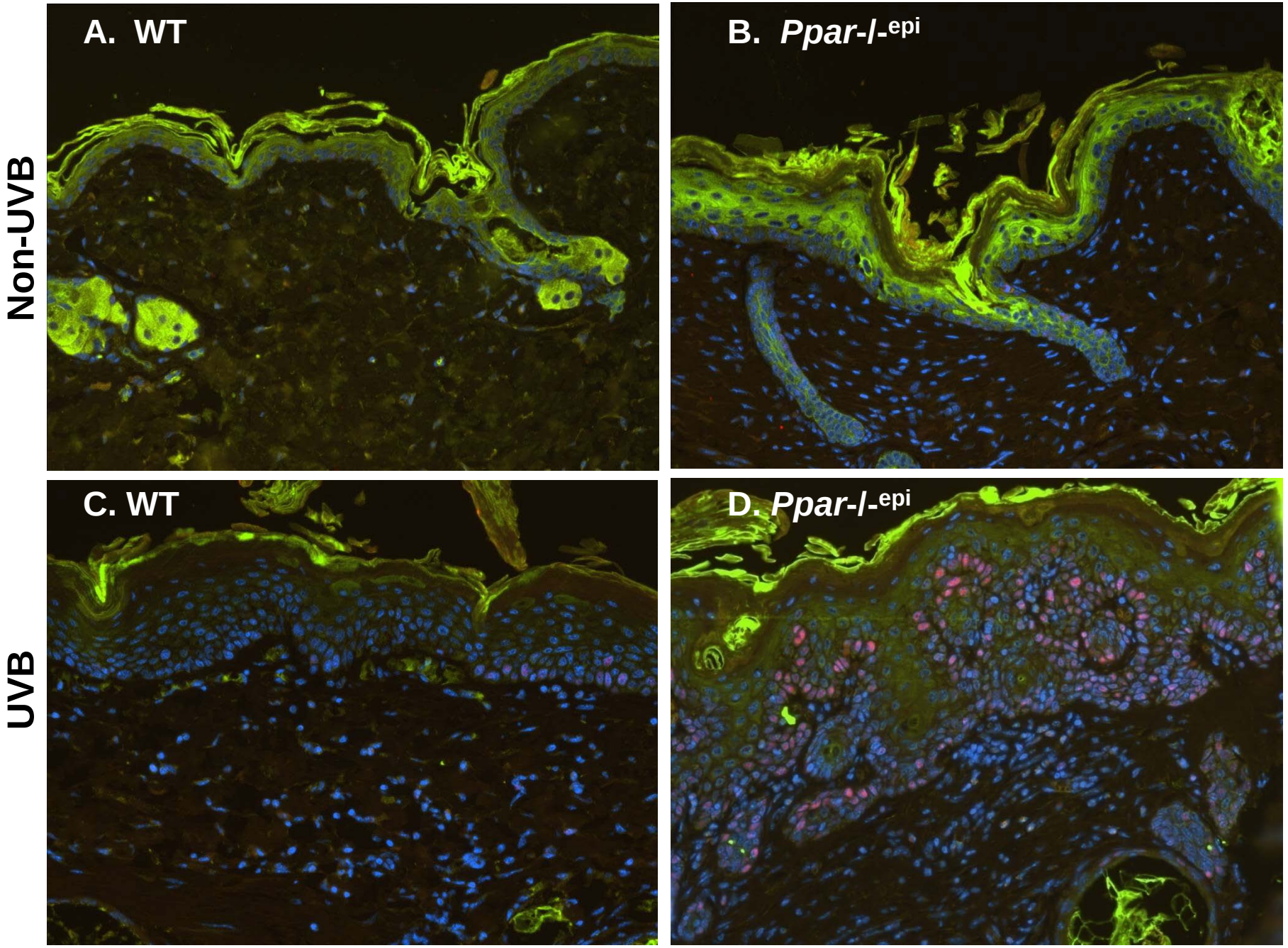

Supplemental figure 2

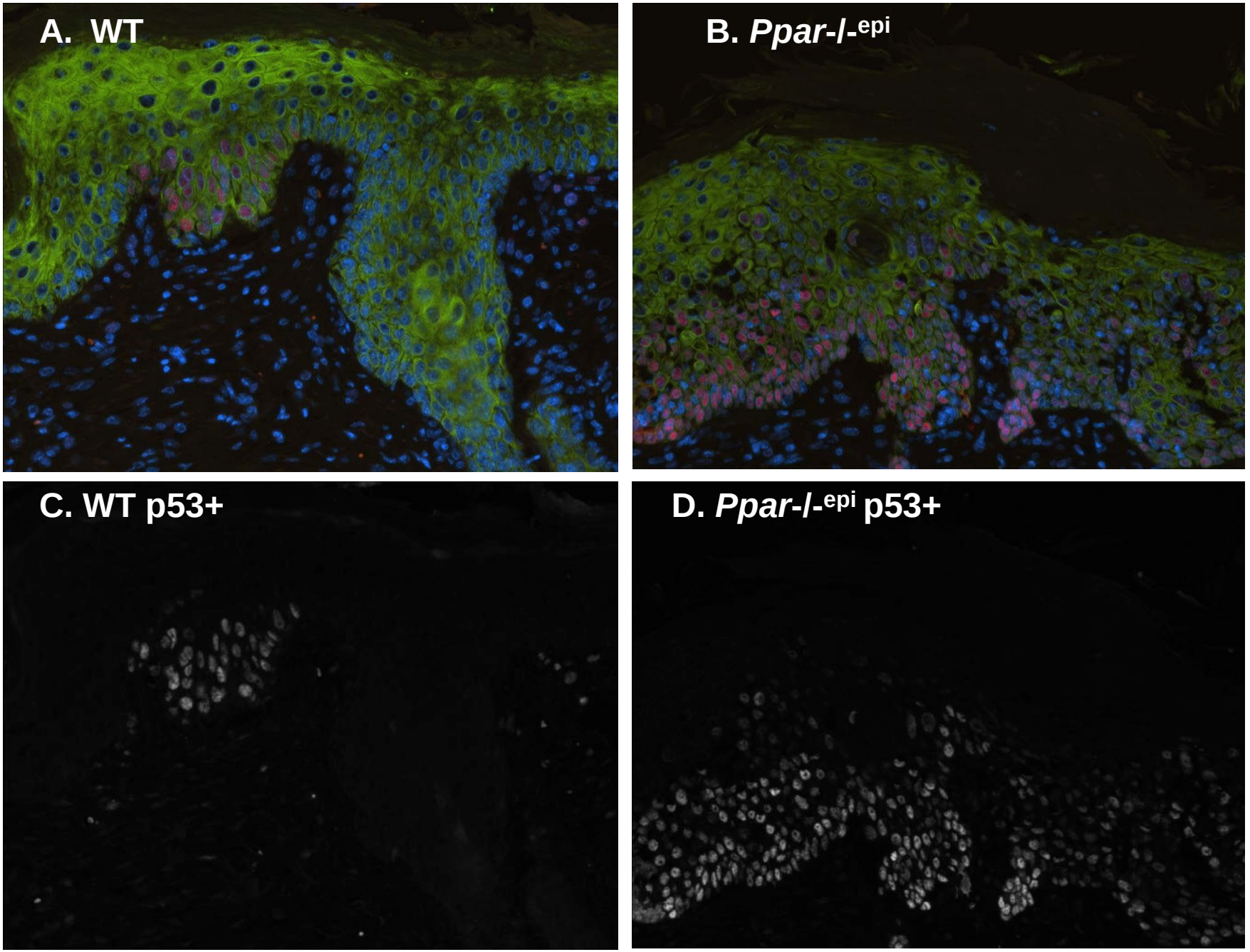

Supplemental figure 3

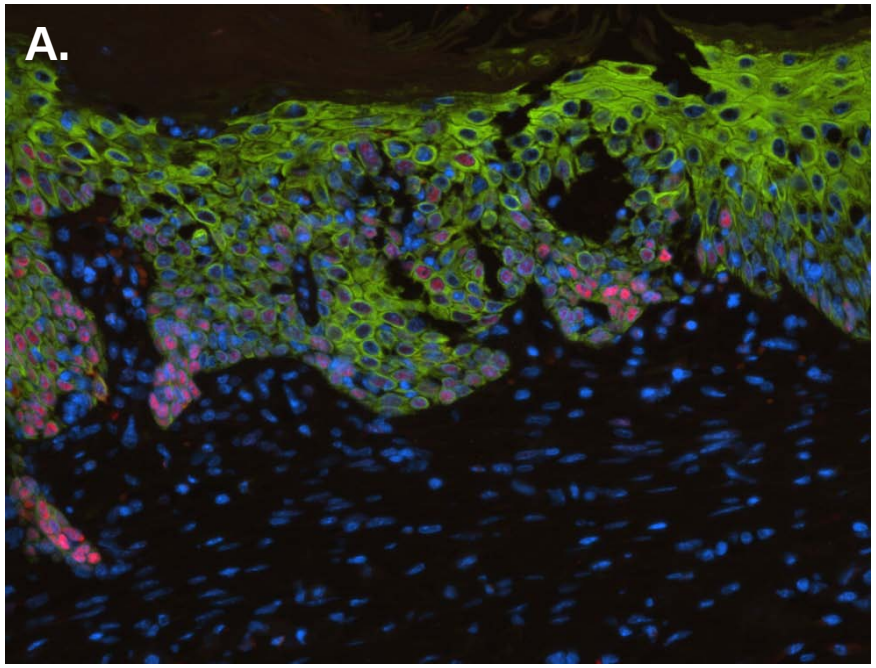

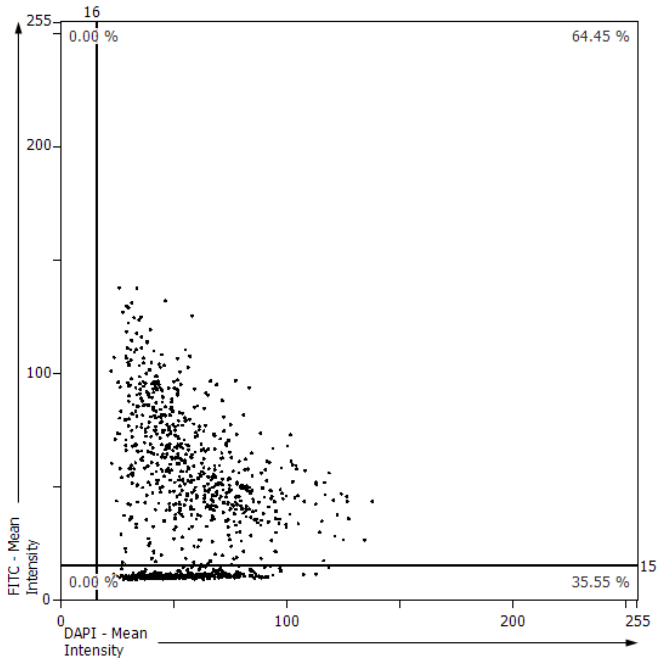

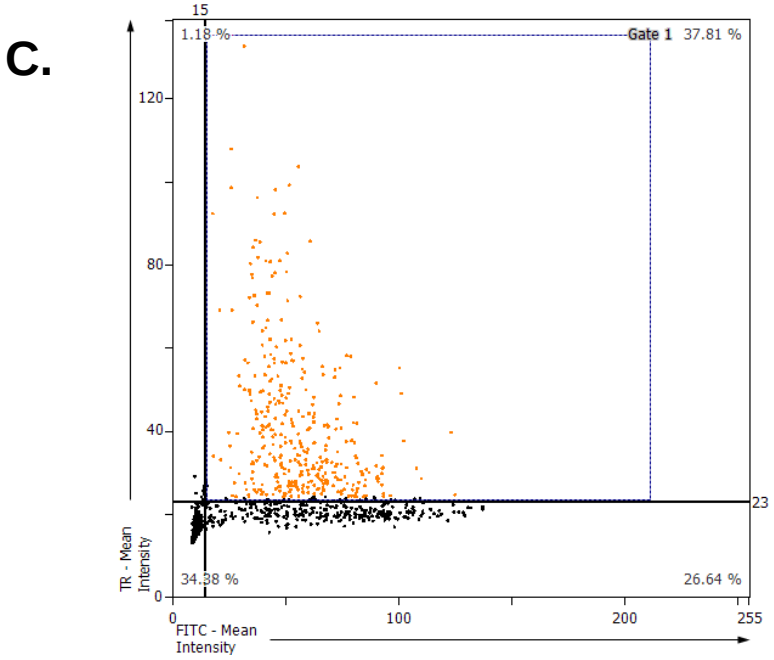

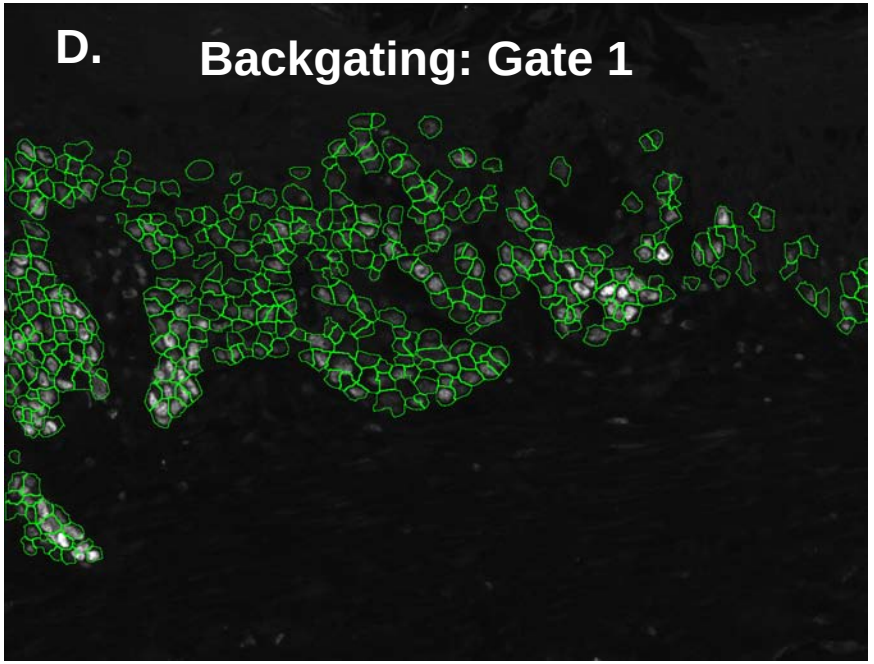

Supplemental Figure 4